

Local electrical stimulation of single adherent cells using three-dimensional electrode arrays with small interelectrode distances

Dries Braeken, Roeland Huys, Danny Jans, Josine Loo, Simone Severi, Frank Vleugels, Gustaaf Borghs, Geert Callewaert and Carmen Bartic

Abstract—In this paper, we describe the localized and selective electrical stimulation of single cells using a three-dimensional electrode array. The chip consisted of 84 nail-like electrodes with a stimulation surface of $0.8 \mu\text{m}^2$ and interelectrode distances as small as $3 \mu\text{m}$. N2A cells were used to compare bipolar stimulation between one electrode in- and one outside the cell on the one hand, and two electrodes in the same cell on the other hand. Selective and localized stimulation of primary embryonic cardiomyocytes showed the possibility to use this chip with excitable cells. The response of the cells to applied electrical fields was monitored using calcium imaging whereas assessment of electroporation was determined following influx of propidium iodide. Arrays of these three-dimensional electrodes could eventually be used as a tool to selectively electroporate the membrane of single cells for genetic manipulation or to obtain electrical access to the inner compartment of the cell.

I. INTRODUCTION

MICROFABRICATION of multi-electrode arrays is offering a growing amount of solutions to various challenges in all fields of the biomedical research. Microelectrode arrays (MEAs) represent a new tool for the evaluation of electrical activity of excitable cells due to the non-invasive contact that allows relatively long-term investigations to be performed [1]. They offer an easy alternative to complex and technically difficult techniques, such as the patch clamp technique, for the recording of electrical activity of various cell types and tissues [2,3].

On the other hand, planar microelectrode chips are used for the electrical stimulation of cells or tissues for long-term potentiation studies in acute brain slices [4] or for the selective poration of the cell membrane in DNA transfection studies. Several groups reported the feasibility of localized electroporation and transfection in adherent cells using MEAs [5,6]. However, MEAs still suffer from several drawbacks. The most important disadvantage is the rather poor electrical coupling of the planar electrode with the cell surface. This leads to a significant loss in the recorded signal-to-noise ratio and a decreased efficiency of electrical stimulation. Also, the large dimensions of the electrodes and

the even larger interelectrode distances on most available MEAs are not suited for single cell experiments.

The electrode-membrane coupling can be improved using three-dimensional electrodes with sizes that are smaller than the cell itself. We reported earlier a strong engulfment of three-dimensional nail-shaped electrodes by the cell membrane and the selective manipulation of excitable cells using these electrodes [7,8]. Small electrode dimensions, however, require active circuitry on the chip to be able to use it for recording of electrical activity of cells. Also, active chips can be upscaled to very large sensing/recording matrices that could result in high-throughput systems.

In this paper, we demonstrate the electrical stimulation of single cells using biphasic voltage pulses between two three-dimensional electrodes located close to each other, creating a local electrical field. Changes in the relative intensity of the fluorescent Ca^{2+} indicator Fluo-4 from stimulated cells were recorded to screen for intracellular $[\text{Ca}^{2+}]$ changes. Electroporation of the membrane was assessed by the influx of the cell-impermeable molecule propidium iodide.

II. METHODOLOGY

A. Fabrication of passive electrode array chip

The fabrication of the micronails is comparable to the method by Huys *et al.* [9] based upon the standard CMOS dual damascene copper process. However, tungsten was used instead of copper to reduce cytotoxicity. Firstly, $3 \mu\text{m}$ HDP oxide is deposited and electrical connections are made by lithography of a dark-field mask followed by etching (400 nm) of the patterns. Next, adhesion layers of 15 nm titanium (Ti) and 10 nm titanium nitride (TiN) were deposited and the pattern was filled by tungsten (W) using chemical vapor deposition. Afterwards, the slack on the topside was removed and planarized by chemical-mechanical polishing (CMP). A diffusion barrier layer of 50 nm SiC was deposited to reduce cytotoxicity. After this, another passivation layer of $3 \mu\text{m}$ oxide was deposited. Conductors in the micronails were fabricated by etching vias of 600 nm wide and $3 \mu\text{m}$ deep through the passivation oxide and the SiC barrier. The vias were filled with a diffusion barrier layer of tantalum nitride (15 nm), an adhesion layer of 15 nm Ti and 10 nm TiN, and tungsten. Again, the slack on the topside was removed and planarized by CMP. The electrodes (shown in Figure 1B) were made by first depositing 100 nm TiN and then performing lithography with a light-field mask centered around the tungsten vias, followed with a TiN etch, resulting in planar electrodes. The nails were formed by lithography with a light-field mask of

Manuscript received April 7, 2009. This work was supported in part by the Seventh Framework Programme European project 'Brain Storm' (215486).

D. Braeken, R. Huys, D. Jans, J. Loo, S. Severi, F. Vleugels, S. Borghs and C. Bartic are with the Interuniversity MicroElectronics Center (IMEC), Kapeldreef 75, 3001 Leuven, Belgium (corresponding author: phone: +32-16-288942; e-mail: dries.braeken@imec.be).

D. Jans and G. Callewaert are with the Neurophysiology Lab, Subfaculty Kortrijk, Katholieke Universiteit Leuven, E. Sabbelaan 53, 8500 Kortrijk, Belgium.

circles of 1.2 μm centered around the TiN electrodes, followed by a time-controlled oxide etch to remove the field oxide, resulting in nails of 500 nm to 1 μm high, with flat TiN electrodes on top, electrical connection in the shaft (W) insulated by SiO_2 , and planar connections on the bottom. Finally, the chips were diced and then packaged by flip-chip and epoxy-underfill.

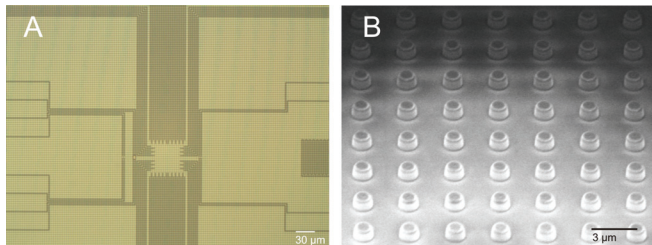


Fig. 1. A) Bright field image of the complete nail electrode chip with the active area in the center. B) SEM image of the nail electrodes on the active area.

B. Cell culturing

Neuroblastoma (N2A) cells were purchased from ATCC (CCL-131). Cells were subcultured in DMEM-F12 medium, containing 10% fetal calf serum (FCS), 1% non-essential amino acids, 2% PenStrep and 1% glutamax (Invitrogen, Belgium). For the differentiation medium, FCS was omitted. Cells were cultured on ethanol-sterilized chips and seeded at a density of 60,000 cells/ml. After 2 days in culture, the medium was changed to differentiation medium to stop cell division and promote neuronal differentiation.

Hearts of 16-day old Wistar rat embryos were removed under sterile conditions and placed in Ca^{2+} - and Mg^{2+} -free HBSS solution as described previously [10]. After removing excess blood, the heart was chopped in small fragments of 1 mm^2 pieces and collected in a Falcon tube. Trypsin-EDTA (0.05%) was then added to the tube. After 8 minutes of incubation at 37°C, the supernatant was discarded. The enzymatical dissociation was done by addition of DNase Type II solution (10,000 units/ml) that was incubated for 3 minutes at 22°C. Next, 2.5 ml of trypsin-EDTA was added and incubated for 8 minutes at 37°C. The supernatant was collected and added to Hams F10 containing 0.5% insulin, transferrin and selenite solution (ITS) and 33% fetal calf serum and kept on ice. The collected cells were then centrifuged for 10 minutes at 4°C and 200 g and resuspended in Ham's F10 medium containing 0.5% ITS and 5% FCS. For the remaining tissue, this trypsinization step was repeated at least 5 times. The collected cell suspensions were then seeded on 30 mm culture dishes and incubated for 70 minutes at 37°C and 5% CO_2 for differential adhesion. After this plating step, the cells were collected and centrifuged for 10 minutes at 22°C and 200 g. The pellet was then resuspended in cell medium. The cells were eventually plated on uncoated devices at cell densities of 40,000 cells/ml.

C. Calcium imaging and PI monitoring

Fluo-4 AM was dissolved in DMSO containing 20% (w/v) Pluronic to obtain a final concentration of 5 μM Fluo-4.

Propidium iodide (PI) was then added to this same solution to obtain a final concentration of 1 $\mu\text{g/ml}$. The cells were first transferred to Ca^{2+} -free KREBS solution (135 mM NaCl; 5.9 mM KCl; 2 mM EGTA; 1.2 mM $\text{MgCl}_2 \cdot 6\text{H}_2\text{O}$; 11.6 mM HEPES; 11.5 mM glucose; pH 7.3) and incubated with the Fluo-4 and PI solution for 30 minutes at 37°C. Afterwards, the cells were rinsed with a 1.5 mM Ca^{2+} KREBS solution (135 mM NaCl; 5.9 mM KCl; 1.5 mM CaCl_2 ; 1.2 mM $\text{MgCl}_2 \cdot 6\text{H}_2\text{O}$; 11.6 mM HEPES; 11.5 mM glucose; pH 7.3). Cells were then excited at 488 nm (Fluo-4) and 555 nm (PI) using a CellR Live Imaging system coupled to an upright microscope (BX51, Olympus). Data were processed using the CellR software.

D. Electrical stimulation set-up

Bipolar electrical stimulation was performed by the connection of two nail electrodes with a local battery-powered opamp operating in unity-gain feedback mode. The culture medium was not connected to a reference electrode, so charge displacements in the culture medium due to the stimulation pulses were only occurring between the electrodes. Pulses were generated with the Clampex software using episodic stimulation of biphasic pulse trains with a pulse width of 200 μs to 1 ms, and amplitudes from 100 mV to 2 V, with increasing amplitudes. The signals are generated by the acquisition system Digidata 1440 from Axon Instruments, Molecular Devices (Figure 2).

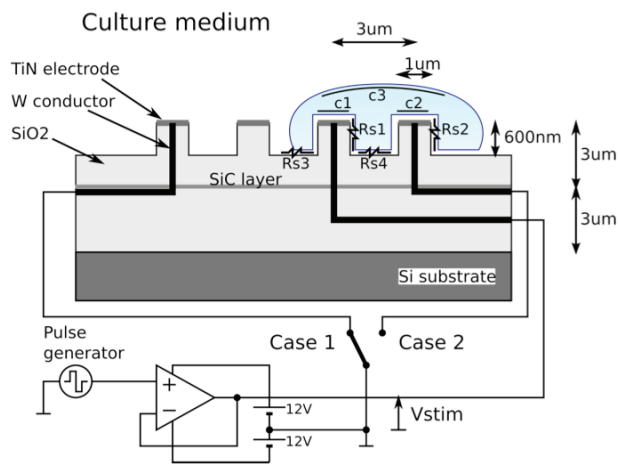


Fig. 2. Schematic overview of the experimental set-up and cross-section of the chip. Two cases are used: in Case 1, the P-electrode is underneath the cell and the N-electrode is connected to free culture medium; in Case 2, both electrodes are underneath the cell.

III. RESULTS AND DISCUSSION

A. Electrical stimulation of a single cell with one electrode underneath the cell - Case 1

To determine the effect of electrical stimulation in the situation when a cell was positioned on top of one nail electrode, we seeded N2A cells on the chip surface and connected one nail electrode underneath the cell and one nail electrode outside the cell, indicated by arrows in Figure 3A, (1-2). Increasing biphasic voltage pulses (pulse width = 200 μs) were applied between the two electrodes to stimulate the

cell that was positioned in between the electrical field. Figure 3 shows increasing voltage pulses applied to the electrodes while monitoring the intracellular $[Ca^{2+}]$. At amplitudes around 1.5 V, the cell showed an increase in relative $[Ca^{2+}]$ ($\Delta F/F_0$). Further stimulation with the same voltage pulse caused again an increase of the intracellular $[Ca^{2+}]$, however with a smaller amplitude. Directly after the experiment, cells were loaded with PI to validate the existence of pores in the membrane. Figure 3E shows that PI fluorescence remained non-existent after stimulation, indicating that, if pores were formed in the membrane, they were small and not permeable to PI. Propidium iodide is a small molecule (MW=668 Da), which is commonly used to determine poration of membranes for electroporation purposes [11].

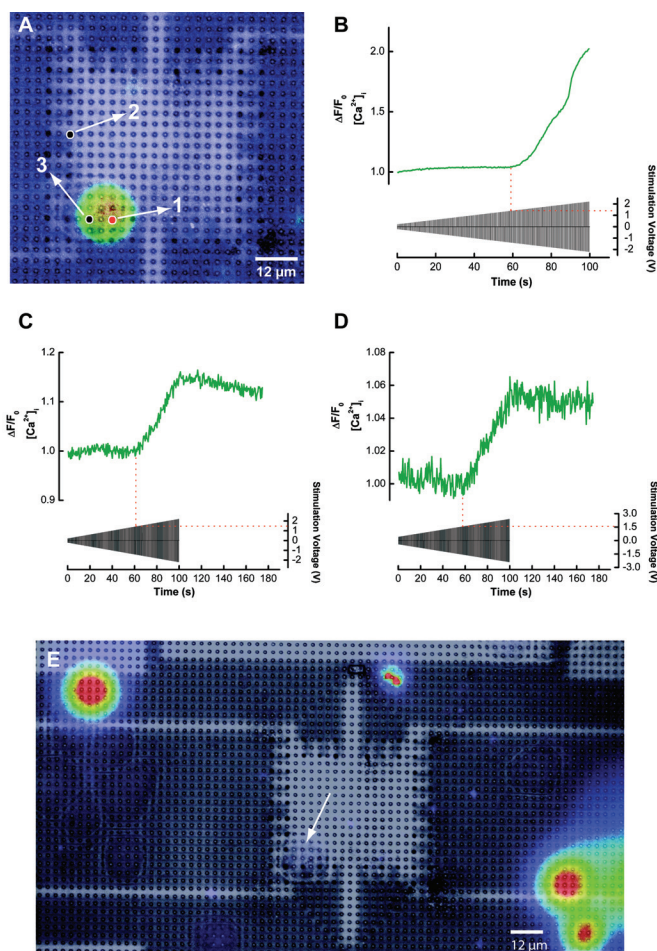


Fig. 3. Localized electrical stimulation of a N2A cell on the passive electrode array. A) Pseudo-fluorescence image of Fluo-4 loaded cell merged with a bright field image of the active area of the chip and the electrodes used for stimulation (1-3). B-C-D) Relative intracellular $[Ca^{2+}]$ change ($\Delta F/F_0$) in the cell during electrical voltage stimulation. E) PI staining after stimulation. The arrow indicates the position of the stimulated cell.

B. Electrical stimulation of a single cell with two electrodes underneath the cell - Case 2

After the experiment shown above, two nail electrodes underneath the cell were connected (Figure 3A, 1-3). Increasing voltage pulses were applied while monitoring simultaneously the changes in relative fluorescence in intracellular $[Ca^{2+}]$ and PI. Figure 4 shows the response of the cell during voltage stimulation. Whereas the relative $[Ca^{2+}]$ strongly decreased starting from amplitudes around 0.2 V, PI fluorescence increased, indicating the formation of large pores in the cell membrane. The image shows the PI staining of the cell on top of the chip surface after the experiment.

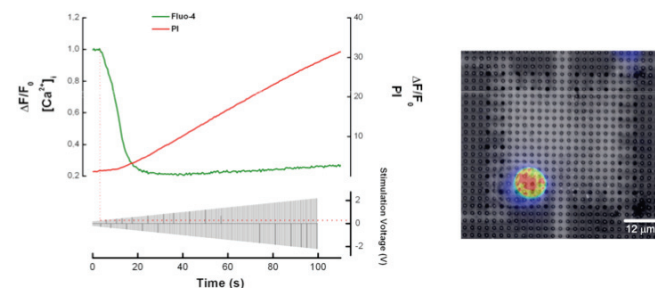


Fig. 4. Relative change in fluorescence of Fluo-4 (green) and PI (red) upon voltage stimulation between two nail electrodes underneath the cell. The image shows an overlay of a bright field image of the active area and the PI staining of the cell.

In the experiments shown above, two cases were tested: bipolar stimulation between one electrode in- and one outside of the cell (Case 1) and bipolar stimulation between two nails inside the same cell (Case 2). In Case 1, the maximum voltage across the membrane (Figure 2, c1) was determined by a capacitive division between the cell membrane on top of the electrode (c1) and the cell membrane in contact with the free culture medium (c3) ($V_m = c3/(c1+c3)$). Since the area of c3 was expected to be 100 to 1000 times larger than that of c1 and c2, more than 99% of the maximum voltage was across (c1). This could imply that the intracellular potential cannot be elevated above the threshold level of the cell only by capacitive coupling between the sensor and the cell membrane. However, when pores are formed in the membrane, the coupling is not purely capacitive because a resistive component will shunt the membrane capacitance, which would result in a significant elevation of the intracellular potential towards the threshold for opening of voltage-gated Ca^{2+} channels. The threshold at which voltage electroporation occurs depends on the effectiveness of the coupling between the micronail electrode and the cell membrane, which is mainly determined by the sealing resistance between the electrode and the free culture medium ($R_{s1}+R_{s3}$) and the area of the cell membrane on top of the electrode (c2). We observed this threshold voltage to be between around 1.5-1.6 V with pulse widths of 200 μs to 1 ms. In Case 2, the maximum voltage across either membrane (c1) or (c2) was determined by the capacitive ratio between the two, so the threshold at which point electroporation

occurs was determined by the smallest value of (c_1 , c_2) and by the total sealing resistance ($R_{s1}+R_{s2}+R_{s4}$), so the largest value of (R_{s1} , R_{s2}) will be dominant. We expect a large variation on the quality of the electrode-cell membrane coupling, but in Case 2, the best coupling of both electrodes determines the minimal threshold voltage for electroporation. This implies that Case 2 should show a lower average threshold voltage. In order to prove this hypothesis, however, additional experiments will have to be performed.

C. Localized electroporation of embryonic cardiomyocytes

Next, primary embryonic cardiomyocytes were chosen because they are interesting cells for the monitoring of intracellular Ca^{2+} processes, and they show more potential for biomedical research purposes than immortalized cell lines. Only cells that showed no spontaneous activity were selected for the experiments. Figure 5B shows repetitive stimulation of a cardiomyocyte that was positioned on top of one nail electrode; the second electrode was located outside the cell (Figure 5A, 1-2). The relative Ca^{2+} signal initially showed a fast upstroke followed by a decrease leading to a new baseline level. Applying an identical voltage pulse train a second and third time showed again an initial increase in the Ca^{2+} level, which returns to the baseline.

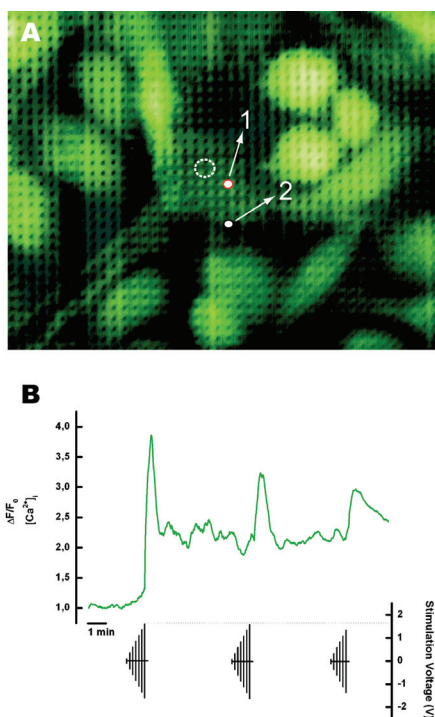


Fig. 5. Localized electrical stimulation between two electrodes (arrows 1-2) of a single cardiomyocyte cultured on top of the nail electrode chip. The circle indicates the region where the fluorescence was measured.

In the case of excitable cardiomyocytes, it is also not clear whether the increase in the relative Ca^{2+} concentration is only due either to formation of pores in the membrane or the opening of voltage-gated ion channels, which both cause influx of extracellular Ca^{2+} . Because the Ca^{2+} level did not

come back to its original baseline level, we assume that small pores existed that remain open for a longer time, leading to residual membrane leakiness [12].

IV. CONCLUSIONS

We fabricated a passive three-dimensional electrode array with a CMOS-compatible process flow in order to implement nail-shaped structures directly onto active circuitry. This implies the possibility of in-situ amplification of the signals or closed-loop electrical stimulation with the chip. Experimental data showed the possibility of localized and selective stimulation of excitable and non-excitable cells.

V. ACKNOWLEDGMENT

This work was funded by the Seventh Framework Programme European project 'Brain Storm' (215486).

REFERENCES

- [1] A. Stett, U. Egert, E. Guenther, F. Hofmann, T. Meyer, W. Nisch and H. Haemmerle, "Biological application of microelectrode arrays in drug discovery and basic research," *Anal. Bioanal. Chem.* 377 (3): 486-495, 2003.
- [2] L. Berdondini, P. Massobrio, M. Chiappalone, M. Tedesco, K. Imfeld, A. Maccione, M. Gandolfo, M. Koudelka-Hep and S. Martinoia, "Extracellular recordings from locally dense microelectrode arrays coupled to dissociated cortical cultures," *J. Neurosci. Meth.* 177 (2): 386-396, 2009.
- [3] J. K. Y. Law, C. K. Yeung, B. Hofmann, S. Ingebrandt, J. A. Rudd, A. Offenhausser and M. Chan, "The use of microelectrode array (MEA) to study the protective effects of potassium channel openers on metabolically compromised HL-1 cardiomyocytes," *Physiol. Meas.* 30 (2): 155-167, 2009.
- [4] Y. Berdichevsky, H. Sabolek, J. B. Levine, K. J. Staley and M. L. Yarmush, "Microfluidics and multielectrode array-compatible organotypic slice culture method," *J. Neurosci. Meth.* 178 (1): 59-64, 2009.
- [5] Y. C. Lin, M. Li and C. C. Wu, "Simulation and experimental demonstration of the electric field assisted electroporation microchip for in vitro gene delivery enhancement," *Lab Chip* 4 (2): 104-108, 2004.
- [6] T. Jain, J. and Muthuswamy, "Microelectrode array (MEA) platform for targeted neuronal transfection and recording," *IEEE Trans. Biomed. Eng.* 55 (2): 827-832, 2008.
- [7] B. Van Meerbergen, J. Loo, R. Huys, T. Raemaekers, K. Winters, D. Braeken, Y. Engelborghs, W. Annaert, G. Borghs and C. Bartic, "Functionalized microneedles for enhanced neuronal adhesion," *J. Exp. Nanosci.* 3 (2): 147-156, 2008.
- [8] D. Braeken, D. Jans, D. Rand, R. Huys, B. Van Meerbergen, J. Loo, G. Borghs, G. Callewaert and C. Bartic, "Local Electrical Stimulation of Cultured Embryonic Cardiomyocytes with Sub-micrometer Nail structures," 30th Annual Internat. Conf. of the IEEE Eng. Med. Biol. Soc., 1-8: 4816-4819, 2008.
- [9] R. Huys, D. Braeken, B. Van Meerbergen, K. Winters, W. Eberle, J. Loo, D. Tsvetanova, C. Chen, S. Severi, S. Yitzchaik, M. Spira, J. Shappir, G. Callewaert, G. Borghs and C. Bartic, "Novel concepts for improved communication between nerve cells and silicon electronic devices," *Solid-State Elect.* 52(4): 533-539, 2008.
- [10] M. Krause, S. Ingebrandt, D. Richter, M. Denyer, M. Scholl, C. Sprossler and A. Offenhausser, "Extended gate electrode arrays for extracellular signal recordings," *Sens. Actuat. B Chem.* 70 (1-3): 101-107, 2000.
- [11] K. Maswiat, D. Wachner and J. Gimsa, "Effects of cell orientation and electric field frequency on the transmembrane potential induced in ellipsoidal cells," *Bioelectrochem.* 74 (1): 130-141, 2008.
- [12] M. N. Teruel and T. Meyer, "Electroporation-induced formation of individual calcium entry sites in the cell body and processes of adherent cells," *J. Neurosci.* 73 (4): 1785-1796, 1997.